

# Diving Deep onto Discriminative Ensemble of Histological Hashing & Class-Specific Manifold Learning for Multi-class Breast Carcinoma Taxonomy\*

Sawon Pratiher<sup>§</sup> and Subhankar Chatteraj<sup>‡</sup>

<sup>§</sup>Department of Electrical Engineering, Indian Institute of Technology Kharagpur, WB, India

<sup>‡</sup>Department of Electronics & Communication Engineering, Techno India University, WB, India

**Abstract**—Histopathological images (HI) encrypt resolution dependent heterogeneous textures & diverse color distribution variability, manifesting in micro-structural surface tissue convolutions. Also, inherently high coherency of cancerous cells poses significant challenges to breast cancer (BC) multi-classification. As such, multi-class stratification is sparsely explored & prior work mainly focus on benign & malignant tissue characterization only, which forestalls further quantitative analysis of subordinate classes like adenosis, mucinous carcinoma & fibroadenoma etc, for diagnostic competence. In this work, a fully-automated, near-real-time & computationally inexpensive robust multi-classification deep framework from HI is presented.

The proposed scheme employs deep neural network (DNN) aided discriminative ensemble of holistic class-specific manifold learning (CSML) for underlying HI sub-space embedding & HI hashing based local shallow signatures. The model achieves 95.8% accuracy pertinent to multi-classification & 2.8% overall performance improvement & 38.2% enhancement for Lobular carcinoma (LC) sub-class recognition rate as compared to the existing state-of-the-art on well known *BreakHis* dataset is achieved. Also, 99.3% recognition rate at 200 $\times$  & a sensitivity of 100% for binary grading at all magnification validates its suitability for clinical deployment in hand-held smart devices.

**Index Terms**—breast cancer; image hash; sub-space learning; discriminative ensemble; deep learning; deep neural networks.

## I. INTRODUCTION

Burgeoning cancer statistics from World Health Organization (WHO) & World Cancer Report (WCR) projects a morbidity rate of 25.2%, 0.5 million mortality [1] & an yearly estimated 1.7 million new cases of BC is registered worldwide [2]. Significant research spanning imaging technique like magnetic resonance (MR), computed tomography (CT), mammography & HI anatomization have been developed for early stage BC prognosis through precision medicine initiative, but HI analysis is taken as the "gold standard" due to its rich encoded histological morphology, substantiating abnormal cellular activity. Additionally, deformation dynamics of these spatial tissue textures allows more specific characterizations from a diagnostic perspective [3] & aid pathologists to control growth & metastasis of tumor cells & devise therapeutic clinical schedules specific particular sub-classes.

However, owing to ubiquitously abundant inhomogeneous morphology & complex intricate spatial correlations in the underlying inter-weaved biological tissue fabric of biopsy samples [4], automated machine vision for robust & accurate multi-class BC detection is still a challenging task & eludes researchers. Manual BC multi-classification by pathologist is arduous & requires domain expertise with interpretations being subjective in nature. An automated computer aided diagnostic

(CAD) system overcome these challenges & assist clinicians in reliable diagnosis [5-6] by reducing their workload & avoid erroneous diagnosis. Further, practical CAD systems face challenges of inefficient hand-crafted feature engineering, which is computationally intensive & time consuming. Secondly, optimal supervised feature selection for accurate BC identification via image segmentation & identification of primitives like nuclei deformation, tubule formation, lymphocytes presence etc., [7] & high resolution HI analysis is computationally expensive requiring costly high performance computation, which is generally not available in developing countries. Fig. 1 shows representative Hematoxylin & Eosin (H&E) stained fine-grained multi-class biopsy tissue slides acquired @400 $\times$  magnification (Taken from *BreakHis* [8]). Subtle inter-class & intra-class variability w.r.t., contrast & textures are evident.

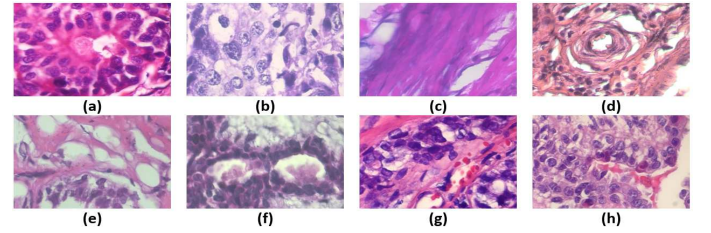


Figure 1. (a) Ductal carcinoma (DC), (b) Lobular carcinoma (LC), (c) Mucinous carcinoma (MC), (d) Papillary carcinoma (PC), (e) Adenosis, (f) Fibroadenoma, (g) Tubular adenoma (TA), (h) Phyllodes tumor (PT). (a) to (d) & (e) to (g) corresponds to malignant and benign class respectively.

To resolve these challenges, a reliable & more accurate practical method for BC multi-classification via DNN is developed. The proposed method discards feature engineering & employs end-to-end training of deep discriminative ensemble of holistic HI CSML & local high-level to low-level semantic hierarchical hash signatures followed by softmax layer for classification. The model is validated with 7909 HI to demonstrate its potency for deployment in clinical settings on generic processors, while experimental results outperforms the existing state-of-the-art. The main contributions can be recapitulated as:

- A novel DNN for real-time BC multi-classification framework, as shown in Fig. 2, is explored. The model yields the highest state-of-art recognition rate with reduced computational time & complexity.
- The scheme leverages the intra-class morphological similarities & inter-class dissimilarities of the hierarchical feature space in a discriminative manner via deep ensemble of CSML & heterogeneous hash signatures.

\*This paper is submitted in IEEE International Conference on Acoustics, Speech, and Signal Processing (IEEE ICASSP), Brighton, UK, 2019

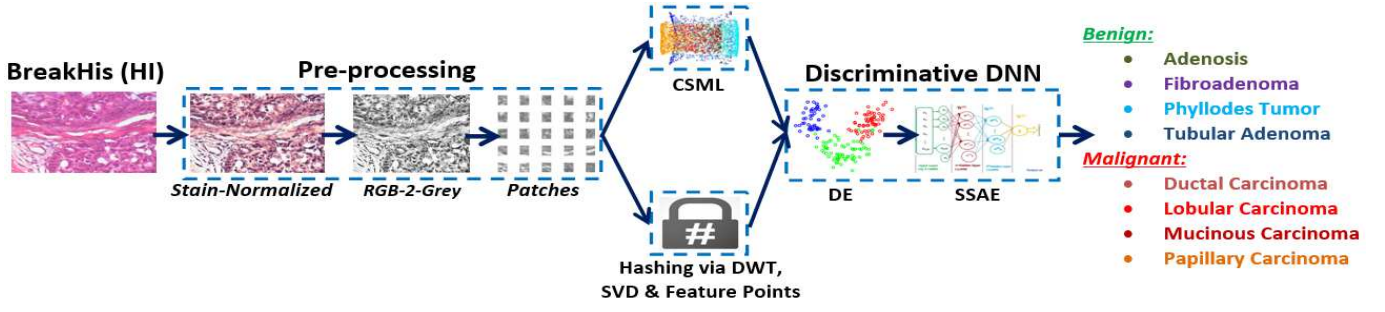


Figure 2. Stages of integrated pipeline: pre-processing, CSML & HI hash extraction, discriminative ensemble & DNN learning.

## II. MATERIALS & PRIOR WORK

### A. BreakHis Dataset

The proposed BC multi-classification method is examined on publicly available large-scale *BreaKHis* dataset [8] containing 7,909 HE stained microscopic images from surgical biopsy (SOB) breast tumors, taken from 82 patients & collected at multiple magnification factor of:  $40\times$ ,  $100\times$ ,  $200\times$  &  $400\times$ . The images are of  $700\times 460$  pixels dimension with 24-bit color depth in 3-channel RGB (Red-Green-Blue) format. Table 1 summarizes the distribution different histological sub-types. *BreaKHis* details can be traced from [8].

Table I  
*BreaKHis* DISTRIBUTION W.R.T CLASS, SUB-CLASSES & MAGNIFICATION

Class	SC	Magnification Factor				Total	Patient
		$40\times$	$100\times$	$200\times$	$400\times$		
M	DC	864	903	896	788	3451	58
	LC	156	170	163	137	626	
	MC	205	222	196	169	792	
	PC	145	142	135	138	560	
B	A	114	113	111	106	444	24
	F	253	260	264	237	1014	
	TA	109	121	108	115	453	
	PT	149	150	140	130	569	
Total		1995	2081	2013	1820	7909	82

### B. Prior Art using *BreaKHis*

Significant works are concentrated around binary classification of benign & malignant classes. Over the past few years researches have broadly investigated on optimal feature engineering & deep learning based architectures. These can be found from the works of Spanhol et al., [8], convolution neural network (CNN) with fusion rule (FR) [13], multiple feature vector (MFV) & transfer learning [10], ensemble classifier (EC) of shallow features by Gupta et al., [9], deep CNN by Wei et al., [15], magnification specific multiple CNN models by Das et al., [11] & vector of locally aggregated descriptors (VLAD) on Grassmann manifold (GM) by Dimitropoulos et al., [12]. Efficacy of ConvNet based fisher vector (CFV) & Gaussian mixture model (GMM) by Song et al., [14], whole slide imaging (WSI) using multiple instance learning (MIL) based CNN in by Das et al [16]. A exhaustive comparative survey on the *BreaKHis* dataset can be traced from Table III.

Whereas, studies concerning multi-classification of sub-classes for clinical diagnosis or prognosis is done by Han Zhongyi et al., using class structured deep CNN (CSD-CNN) model [15] & Bardou et al. using CNN based approach [17]. Multi-classification research comparison can be found in Table IV & V.

## III. METHODOLOGY & RELATED THEORY

### A. Experiment Design: Deep Discriminative Ensemble of Histological Hashing & Class-Specific Manifold Learning

Recently, DNN have shown efficacy in achieving state-of-the-art performance in diverse research problems spanning medical imaging [4], natural language processing (NLP) & speech processing. Here, we propose to use stacked sparse autoencoder (SSAE) based DNN [21] for robust BC multi-classification. Fig. 2 highlights the workflow. Our model pipeline consists of three main stages: Pre-processing stage for stain normalization, & overlapping & optimal patch segments of specific size are generated for subsequent tissue index profile abstraction. Thereafter, class-specific manifold learning (CSML) of different histological sub-types are comprehended for nonlinear dimensionality reduction (NLDR). NLDR distillates discriminative low-dimensional structures pertinent to particular sub-class hidden in high-dimensional HI. Via feature-space geometry constraints, CSML preserves the intrinsic quasi-isometric geometry & local contour connectivity of HI point-cloud within tolerable limits, which is very much crucial for diagnosis. Thereafter, different hash signature obtained via discrete wavelet transform (DWT), singular-value decomposition (SVD) & perceptual feature-points augments the local shallow statistical HI descriptors. The holistic CSML & Hash vectors are fused in a discriminative fashion, which contemplates class structure based feature fusion. The ensemble discriminative super feature vectors are fed to SSAE for learning deep features & classification thereof.

### B. Class-Specific Manifold Learning (CSML)

CSML is envisaged via Landmark Isomap (L-ISOMAP) aide Eigen sub-space estimation of a particular histological sub-type. For a vectorized HI point-cloud of  $Y$  data-points, arbitrarily  $m$  ( $m \ll M$ ) points are selected as Landmarks. Euclidean distance based embedding of the input data using  $m$  landmark points are selected from  $Y$  & followed by multi-dimensional scaling (MDS) using the  $m \times m$  matrix  $G_{m,M}$  of

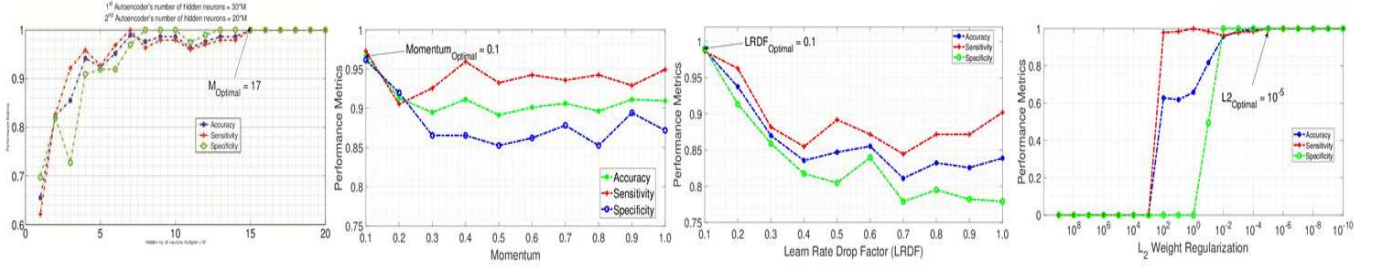


Figure 3. Hyper-parameter tuning in DNN. (a) hidden size, (b) momentum, (c) learn rate drop factor, (d)  $L_2$  weight regularization

geodesic distances for each landmark pair to compute the low dimensional feature space. Mathematically, it is given by:

$$m^T(p, q) = -\frac{1}{2} \left( F_{pq}^2 - e_p \frac{1}{m} \sum_l H_{pl}^2 \right), \quad (1)$$

where,  $H^2$  is the means geodesic distance matrix  $H$  is element-wise squared &  $e_p$  is the Eigen vector with zero Eigen value. Details can be traced from [22].

### C. Histological Hashing for Local Signatures

Rudimentary details can be found in the references given [27]. Histological image hashing encodes locality reference & inherent neighbourhood connectivity of the underlying HI manifold topography. Here, we have used the following hash signatures:

1) *Discrete Wavelet Transform (DWT) Based Image Hash*: Computes robust & compact hash via 2D DWT on HI, which decomposes into four sub-bands namely LL, LH, HL and HH. Edge/high frequency information is realized in LH, HL & HH while coarse stable low-frequent coefficients is perceived in LL sub-bands of the DWT coefficients [23].

2) *Hashing Via Singular Value Decomposition (SVD)*: Robust tolerance to small rotational changes until 10 & is translation in-variance & incorporates low rank approximation of original normalized sub-image of HI & non-correlated directional feature space encoding [28].

3) *Feature Point Based Image Hashing*: Statistical image features like Harris corner detector, Hessian affine, maximally stable extremal region (MSER) detector & feature points based on end-stopping behavior like end-stopped Wavelets such as Morlets preserves the significant image geometry feature points of 2-D HI pixels & map them to 1-D feature vector which is compressed to generate the hash vector [24].

### D. SSAE aided DNN Training & Hyper-parameters Tuning

Discriminative feature ensemble of holistic CSML & shallow hash signatures is fused via discrimination correlation analysis [25]. Stacked Sparse Autoencoder (SSAE) [26] involves optimal parameter  $\theta = (V, a_k, a_y)$  computation by minimizing the error between input and output & rudimentary details can be traced from [21]. The model is trained on generic AMD FX-8320 Octa-core system with 3.50 GHz processor and 16GB RAM. Fig 3 shows hyper-tuned optimal SSAE parameters. A maximum epoch of 500 & number hidden layer neurons in the first and second autoencoders (AE) are kept at 500 & 300 respectively. Further,  $L_2$  weight

regularization, sparsity regularization & sparsity proportion in the two AE are set to 0.001, 4 & 0.15. 'tanh' activation function (AF) in the hidden units is followed by fully connected layer & softmax layer, where 'tanh' AF is used due to its robust tolerance to approximate intrinsic manifold non-linearity & extraction of mutual dependence for further segregation thereof. Stochastic gradient descent (SGD) based back propagation algorithm with learning rate  $10^{-4}$ , piecewise learning rate schedule, random initial weights drawn uniformly from  $[-0 : 1; 0 : 1]$ , momentum of 0.6,  $L_2$  weight regularization of 0.2, gradient decay factor of 0.2, learning rate drop period (LRDP) of 5 is used during the training phase. The weights (W) & bias (b) are updated as

$$W_l = W_l - \eta \frac{\partial}{\partial W_l} (W, b; X, t) = B_l W_l - \eta \frac{\partial}{\partial B_l} (W, B; X, t) \quad (2)$$

where,  $W_l$  represents the weights,  $B_l$  represents the  $l^{th}$  layer bias,  $\eta$  is learning rate, (X, t) is the mini-batch comprising of 'm' training samples. In order to eschew model over-fitting, bias minimization & skewed parameter learning during the training phase, the data is randomly partitioned into training, validation & test set in the ratio 60:20:20. Typically, 2597.31 sec is required for complete one set of training.

## IV. RESULTS AND DISCUSSION

The adequacy of the proposed method is evaluated in terms of standard evaluation metrics i.e., classification accuracy (AC), sensitivity (SN) & specificity (SP). Experimental results for both binary & multi-classification are compared with state-of-the-art techniques on same benchmark *BreCaHis* dataset.

Table II  
RESULTS FOR BINARY CLASSIFICATION. PM = PERFORMANCE METRICS

Class	PM (%)	Magnification Factor			
		40X	100X	200X	400X
Binary	AC	99.1	98.7	<b>99.3</b>	98.4
	SN	<b>100</b>	<b>100</b>	<b>100</b>	<b>100</b>
	SP	98.3	97.9	<b>98.5</b>	96.8

### A. Grading Tumor Malignancy: Binary Classification

Initially, binary classification of BC into benign & malignant classes is done to ensure its competence in coarse HI characterization. Table II highlight performance measure of the experimental results for different magnification factors.



100% sensitivity for all magnification factor ensures that all malignant classes are recognized correctly. As such, pathologist may invest more time for identifying benign cases with our system & demonstrates the effectiveness of the DNN model to learn deep malignancy biomarkers for discriminative HI grading. Table III gives comparative evaluation with the state-of-the-art methods which have been developed in recent years [8-20]. It is worth mentioning that our proposed method outperforms all previous used methods in terms of classification accuracy with significant enhancement for all magnification factors. Further, our proposed discriminative DNN framework outperforms conventional & visual feature descriptor based approach such LBP [8], VLAD [12] and KAZE [20] & also surpasses even recent CNN based methods [10-11][14-16], which is proved to be optimal in analyzing visual imagery. This indicates that our proposed system which is robust in terms of performance & computationally much more efficient as it runs on generic laptops as compared to CNN models, requiring graphics processing unit (GPU).

Table III  
BINARY CLASSIFICATION COMPARISON WITH EXISTING METHOD

Ref, Years	Feature + Method	Performance (%)			
		40X	100X	200X	400X
[13], 2016	CNN, FR	85.6	83.5	82.7	80.7
[8] 2016,	CLBP, SVM	77.40	76.40	70.20	72.80
[9], 2017	C-TID, EC	87.2	88.22	88.89	85.82
[10], 2017	CNN, DeCAF, MFV	84.6	84.8	84.2	81.6
[11], 2017	Deep CNN, FR	94.82	94.38	94.67	93.49
[12], 2017	VLAD, GM	91.8	92.1	91.4	90.2
[14], 2017	I-EM, CFV, CNN, GMM	87.7	87.6	86.5	83.9
[15], 2017	CSDCNN	95.8	96.9	96.7	94.9
[16], 2018	MIL-CNN	89.52	89.06	88.84	87.67
[17], 2018	Dense SIFT, SURF, BOW, LCLC	98.33	97.12	97.85	96.15
[18], 2018	FV, CSE	87.5	88.6	85.5	85.0
[19], 2018	TL, DenseNet	84.72	89.44	95.65	82.65
	CNN, DenseNet	91.90	93.64	95.84	90.15
	MV, XGboost	94.71	95.9	96.76	89.11
[20]	KAZE, BOF, binary SVM	85.9	80.4	78.1	71.1
<b>This Work</b>	<b>CSML, Hashing, DNN</b>	<b>99.1</b>	<b>98.7</b>	<b>99.3</b>	<b>98.4</b>

### B. Multi-classification Performance

We further examine the proposed framework towards multi-class classification of BC to demonstrate its efficacy towards practical use from clinical perspective. Table IV gives comparative evaluation with the state-of-the-art, whereas Table V gives class specific performance accuracy. It is evident that the proposed discriminative DNN framework not only surpasses the state-of-art on the basis of magnification factor but also on the basis of sub-class of HI in terms of recognition rate. To the

best of our knowledge there is very few literature available in multi-class classification of BC from HI. Earlier in the state-of-art, CSDCNN [15] based approach exhibited best recognition rate for multi-class classification but our proposed method surpasses it in all the magnification factor by **3.3%, 1.8%, 2.6%, 3.5%**, for 40 $\times$ , 100 $\times$ , 200 $\times$  & 400 $\times$  magnification. Table V shows that our method surpasses the class-specific recognition rate with high margin & in some case as high as **38.2%** enhancement for Lobular carcinoma (LC) sub-class.

Table IV  
MULTI-CLASSIFICATION COMPARISON WITH EXISTING METHOD

Ref	Feature + Method	Performance (%)			
		40X	100X	200X	400X
[15]	CSDCNN	92.8	93.9	93.7	92.9
[17]	DSIFT + BoW	41.80	38.56	49.75	38.67
	SURF + BoW	53.07	60.80	70.00	51.01
	DSIFT + LLC	60.58	57.44	70.00	49.96
	SURF + LLC	80.37	63.84	74.54	54.70
	DSIFT, BoW + SVM	18.77	17.28	20.16	17.49
	SURF, BoW+ SVM	49.65	47.00	38.84	29.50
	DSIFT, LLC+SVM	48.46	49.44	43.97	32.60
	SURF, LLC+ SVM	55.80	54.24	40.83	37.20
	CNN, SVM-RBF	75.43	71.20	67.27	65.12
<b>This Work</b>	<b>CSML, Hashing, DNN</b>	<b>95.1</b>	<b>95.7</b>	<b>95.8</b>	<b>95.2</b>

Table V  
CLASS-SPECIFIC PERFORMANCE COMPARISON WITH [17]

Class	Ref, years	SC	Magnification Factor			
			40 $\times$	100 $\times$	200 $\times$	400 $\times$
Malignant	[17], 2018	DC	91.51	90.77	91.14	92.74
	<b>This Work</b>	DC	<b>96.7</b>	<b>97</b>	<b>97.6</b>	<b>96.9</b>
	[17], 2018	LC	78.72	54.90	63.27	56.10
	<b>This Work</b>	LC	<b>93.8</b>	<b>94.7</b>	<b>92.8</b>	<b>93.1</b>
	[17], 2018	MC	70.49	82.09	61.02	70.59
	<b>This Work</b>	MC	<b>94.4</b>	<b>95.8</b>	<b>96.6</b>	<b>94.9</b>
	[17], 2018	PC	67.44	83.72	57.50	68.29
	<b>This Work</b>	PC	<b>93.1</b>	<b>95.2</b>	<b>93</b>	<b>93.1</b>
	[17], 2018	A	85.29	79.41	84.85	90.63
Benign	<b>This Work</b>	A	<b>93.5</b>	<b>93.9</b>	<b>97</b>	<b>94.1</b>
	[17], 2018	F	86.84	91.03	91.14	77.46
	<b>This Work</b>	F	<b>95</b>	<b>95.6</b>	<b>94.9</b>	<b>95.1</b>
	[17], 2018	TA	75.56	93.33	76.19	82.05
	<b>This Work</b>	TA	<b>94.5</b>	<b>94.1</b>	<b>94.3</b>	<b>94.4</b>
	[17], 2018	PT	76.19	63.89	62.50	58.82
	<b>This Work</b>	PT	<b>94.4</b>	<b>95.1</b>	<b>95.2</b>	<b>94.7</b>

## V. CONCLUSION

In this work, we introduce a novel deep discriminative ensemble learning CAD for multi-class BC characterization. The method implements deep contextual grading of hybrid holistic-level CSML representations & local hash signatures of HI, thereby, effectively discriminating between benign & malignant sub-classes. The proposed approach was validated using *BreakHis* dataset & experimental results demonstrate better discriminating power in outperforming the existing state-of-the-art. In particular, it shows high specificity towards malignant sub-classes, which can assist pathologists by reducing their heavy workload & arrange optimal therapeutic schedules for further diagnosis or prognosis of benign tissues.

Currently, the method is being escalated to include deeper structures using graph CNN & sequential contextual learning via deep Bi-LSTM & conditional random fields (CRF) with a larger corpus to investigate the diagnostic modality of BC.

## REFERENCES

- [1] Boyle, P., & Levin, B. (2008). World cancer report 2008. IARC Press, International Agency for Research on Cancer.
- [2] [http://www.breastcancerindia.net/statistics/stat\\_global.html](http://www.breastcancerindia.net/statistics/stat_global.html) (Retrieved on 03/03/2018)
- [3] Stenkvist, Björn, et al. "Computerized nuclear morphometry as an objective method for characterizing human cancer cell populations". *Cancer research* 38.12 (1978): 4688-4697.
- [4] Boucheron, Laura E., B. S. Manjunath, and Neal R. Harvey. "Use of imperfectly segmented nuclei in the classification of histopathology images of breast cancer." *Acoustics Speech and Signal Processing (ICASSP)*, 2010 IEEE International Conference on. IEEE, 2010.
- [5] Kowal, Marek, et al. "Computer-aided diagnosis of breast cancer based on fine needle biopsy microscopic images". *Computers in biology and medicine* 43.10 (2013): 1563-1572.
- [6] Lacquet, F. A., et al. "Slide preparation and staining procedures for reliable results using computerized morphology." *Archives of andrology* 36.2 (1996): 133-138.
- [7] M. N. Gurcan, L. E. Boucheron, A. Can, A. Madabhushi, N. M. Rajpoot and B. Yener, "Histopathological Image Analysis: A Review," in *IEEE Reviews in Biomedical Engineering*, vol. 2, pp. 147-171, 2009. doi: 10.1109/RBME.2009.2034865
- [8] Spanhol, Fabio A., et al. "A dataset for breast cancer histopathological image classification." *IEEE Transactions on Biomedical Engineering* 63.7 (2016): 1455-1462.
- [9] Gupta, Vibha, and Arnav Bhavsar. "Breast Cancer Histopathological Image Classification: Is Magnification Important?." *Proceedings of the IEEE Conference on Computer Vision and Pattern Recognition Workshops*. 2017.
- [10] Fabio A. Spanhol, Paulo R. Cavalin y, Luiz S. Oliveira, Caroline Petitjean, and Laurent Heutte, "Deep Features for Breast Cancer Histopathological Image Classification", 2017 IEEE International Conference on Systems, Man, and Cybernetics (SMC).
- [11] Kausik Das, Sri Phani Krishna Karri, Abhijit Guha Roy, Jyotirmoy Chatterjee, Debdoot Sheet "Classifying histopathology whole-slides using fusion of decisions from deep convolutional network on a collection of random multi-views at multi-magnification", 2017 IEEE 14th International Symposium on Biomedical Imaging (ISBI 2017).
- [12] Dimitropoulos K, Barmoutis P, Zioga C, Kamas A, Patsiaoura K, Grammalidis N (2017), "Grading of invasive breast carcinoma through Grassmannian VLAD encoding". *PLoS ONE* 12(9): e0185110. <https://doi.org/10.1371/journal.pone.0185110>
- [13] F. A. Spanhol, L. S. Oliveira, C. Petitjean and L. Heutte, "Breast cancer histopathological image classification using Convolutional Neural Networks," 2016 International Joint Conference on Neural Networks (IJCNN), Vancouver, BC, 2016, pp. 2560-2567. doi: 10.1109/IJCNN.2016.7727519
- [14] Song Y., Chang H., Huang H., Cai W. (2017) "Supervised Intra-embedding of Fisher Vectors for Histopathology Image Classification", *Medical Image Computing and Computer-Assisted Intervention - MICCAI 2017 Lecture Notes in Computer Science*, vol 10435. Springer, Cham
- [15] B. Wei, K. Li, S. Li, Y. Yin, Y. Zheng, Z. Han, "Breast cancer multi-classification from histopathological images with structured deep learning model *Sci Rep*, 7 (2017), p. 4172, <https://doi.org/10.1038/s41598-017-04075-z>.
- [16] Kausik Das, Sailesh Conjeti, Abhijit Guha Roy, Jyotirmoy Chatterjee, Debdoot Sheet, "Multiple instance learning of deep convolutional neural networks for breast histopathology whole slide classification" 2018 IEEE 15th International Symposium on Biomedical Imaging (ISBI 2018).
- [17] D. Bardou, K. Zhang and S. M. Ahmad, "Classification of Breast Cancer Based on Histology Images Using Convolutional Neural Networks," in *IEEE Access*, vol. 6, pp. 24680-24693, 2018. doi: 10.1109/ACCESS.2018.2831280
- [18] Yang Song, Hang Chang, Yang Gao, Sidong Liu, Donghao Zhang, Junen Yao, Wojciech Chrzanowski & Weidong Cai, "Feature learning with component selective encoding for histopathology image classification" 2018 IEEE 15th International Symposium on Biomedical Imaging (ISBI 2018).
- [19] Vibha Gupta, Arnav Bhavsar "Sequential Modeling of Deep Features for Breast Cancer Histopathological Image Classification", *The IEEE Conference on Computer Vision and Pattern Recognition (CVPR) Workshops*, 2018, pp. 2254-2261.
- [20] Sanchez-Morillo D., González J., García-Rojo M., Ortega J. (2018) Classification of Breast Cancer Histopathological Images Using KAZE Features. In: Rojas I., Ortuño F. (eds) *Bioinformatics and Biomedical Engineering. IWBBIO 2018. Lecture Notes in Computer Science*, vol 10814. Springer, Cham.
- [21] Bose, Tulika, Angshul Majumdar, and Tanushyam Chattopadhyay. "Machine Load Estimation Via Stacked Autoencoder Regression." 2018 IEEE International Conference on Acoustics, Speech and Signal Processing (ICASSP). IEEE, 2018.
- [22] H. Shi, B. Yin, X. Zhang, Y. Kang and Y. Lei, "A landmark selection method for L-Isomap based on greedy algorithm and its application," 2015 54th IEEE Conference on Decision and Control (CDC), Osaka, 2015, pp. 7371-7376. doi: 10.1109/CDC.2015.7403383
- [23] Li, Yuenan, and Ping Wang. "Robust image hashing based on low-rank and sparse decomposition." *Acoustics, Speech and Signal Processing (ICASSP)*, 2016 IEEE International Conference on. IEEE, 2016.
- [24] V. Monga and B. L. Evans, "Perceptual Image Hashing Via Feature Points: Performance Evaluation and Tradeoffs," in *IEEE Transactions on Image Processing*, vol. 15, no. 11, pp. 3452-3465, Nov. 2006. doi: 10.1109/TIP.2006.881948
- [25] Haghighat, Mohammad, Mohamed Abdel-Mottaleb, and Wade Alhalabi. "Discriminant correlation analysis for feature level fusion with application to multimodal biometrics." *Acoustics, Speech and Signal Processing (ICASSP)*, 2016 IEEE International Conference on. IEEE, 2016.
- [26] Qi, Yu, et al. "Robust feature learning by stacked autoencoder with maximum correntropy criterion." *Acoustics, Speech and Signal Processing (ICASSP)*, 2014 IEEE International Conference on. IEEE, 2014.
- [27] Ghouti, Lahouari. "Robust perceptual color image hashing using quaternion singular value decomposition." *Acoustics, Speech and Signal Processing (ICASSP)*, 2014 IEEE International Conference on. IEEE, 2014.
- [28] Ghouti, Lahouari. "Robust perceptual color image hashing using quaternion singular value decomposition." *Acoustics, Speech and Signal Processing (ICASSP)*, 2014 IEEE International Conference on. IEEE, 2014.